Impact of an initial energy chirp and an initial energy curvature on a seeded free electron laser: the Green's function

2009 J. Phys. A: Math. Theor. 42 045202

(http://iopscience.iop.org/1751-8121/42/4/045202)

J. Phys. A: Math. Theor. **42** (2009) 045202 (13pp) doi:10.1088/1751-8113/42/4/045202

Impact of an initial energy chirp and an initial energy curvature on a seeded free electron laser: the Green's function

Alberto A Lutman[1], **Giuseppe Penco**[2], **Paolo Craievich**[2] **and Juhao Wu**[3]

[1] University of Trieste, DEEI, 34127 Trieste, Italy
[2] Sincrotrone Trieste, 34012 Trieste, Italy
[3] Stanford Linear Accelerator Center, Stanford University, Stanford, CA 94309, USA

E-mail: alberto.lutman@elettra.trieste.it and jhwu@slac.stanford.edu

Received 21 August 2008
Published 11 December 2008
Online at stacks.iop.org/JPhysA/42/045202

Abstract
In a free electron laser (FEL), the electron bunch energy profile at the undulator entrance can have temporal structures. In this paper, we derive the FEL Green's function for the case of the electron bunch having both energy chirp and energy curvature by solving the coupled Vlasov–Maxwell equations. We give an integral representation as well as an analytic expression for the Green's function. The analytical expression is compared with direct numerical results. Evolution of the Green's function temporal duration and the frequency bandwidth are studied.

PACS numbers: 41.60.Cr, 43.58.Ry

(Some figures in this article are in colour only in the electronic version)

1. Introduction

An x-ray free electron laser (FEL) calls for a high quality electron bunch with a low emittance, a high peak current and a high energy [1]. During the acceleration, bunch compression and transportation, the electron bunch is subjected to the radio frequency curvature and wakefield effects. Thus, the energy profile of the electron bunch coming into the undulator can have a temporal structure. These properties will impact the FEL process in the undulator. In this paper, we derive the Green's function for the case when the electron bunch has an initial energy chirp and an energy curvature. With the Green's function solved, the seeded FEL performance can be formulated as the seed convoluting with the Green's function. Therefore, the impact of the electron bunch initial energy profile on the seeded FEL is ready to be studied. This will be reported in an accompanied paper [2]. The effects of the electron bunch initial energy chirp on the FEL performance and the possible short-pulse generation have been studied for self-amplified spontaneous emission (SASE) FEL [3, 4], and a seeded FEL as well [5, 6]. In the later case, the situation is complicated by the interplay of the electron energy chirp and a possible frequency chirp in the seed. In this paper, we further include the effect from a possible energy curvature in the electron bunch when it enters the undulator. Our study for the first time includes the effect of the seed temporal duration on the over all FEL properties.

The paper is organized as the follows. In section 2, the coupled Vlasov–Maxwell equations are introduced and solved, which gives an integral representation for the FEL Green's function. An analytical expression for the Green's function is also obtained. To check its validity, the analytical expression is compared with the numerical results. The properties of the Green's function is studied in section 3. We conclude the paper with discussions in section 4. Derivation details are given in the appendices.

2. Vlasov–Maxwell analysis for an initial value problem

To analyze the start-up of a seeded FEL amplifier we use the coupled set of Vlasov and Maxwell equations which describe the evolution of the electrons and the radiation fields [7]. Solving this set of equations provides an integral representation for the Green's function.

2.1. Coupled Vlasov–Maxwell equations

We follow the analysis and notation of [3, 5, 7]. Dimensionless variables are introduced as $Z = k_w z, \theta = (k_0 + k_w)z - \omega_0 t$, where $k_0 = 2\pi/\lambda_0, \omega_0 = k_0 c$, and $k_w = 2\pi/\lambda_w$ with λ_0 being the radiation wavelength, λ_w being the undulator period, and c being the speed of light in vacuum. We also introduce $p = 2(\gamma - \gamma_0)/\gamma_0$ as the measure of energy deviation, with γ being the Lorentz factor of an electron in the electron bunch, and γ_0 is the resonant energy which is given by

$$\lambda_0 \approx \lambda_w \frac{1 + \frac{K^2}{2}}{2\gamma_0^2}, \tag{1}$$

for a planar undulator, where the undulator parameter is $K \approx 93.4 B_w \lambda_w$ with B_w being the peak magnetic field in Tesla and λ_w is the undulator period in meter. The electron distribution function is $\psi(\theta, p, Z)$. The FEL electric field is written as $E(t, z) = A(\theta, Z)\,\mathrm{e}^{\mathrm{i}(\theta - Z)}$ with $A(\theta, Z)$ being the slow varying envelope function. The one-dimensional linearized Vlasov–Maxwell equations are

$$\frac{\partial \psi}{\partial Z} + p\frac{\partial \psi}{\partial \theta} - \frac{2D_2}{\gamma_0^2}(A\,\mathrm{e}^{\mathrm{i}\theta} + A^*\,\mathrm{e}^{-\mathrm{i}\theta})\frac{\partial \psi_0}{\partial p} = 0, \tag{2}$$

and,

$$\left(\frac{\partial}{\partial Z} + \frac{\partial}{\partial \theta}\right) A(\theta, Z) = \frac{D_1}{\gamma_0}\,\mathrm{e}^{-\mathrm{i}\theta} \int \mathrm{d}p\, \psi(\theta, p, Z), \tag{3}$$

where in SI units,

$$D_1 = \frac{e a_w n_0 [JJ]}{2\sqrt{2} k_w \varepsilon_0}, \qquad \text{and} \qquad D_2 = \frac{e a_w [JJ]}{\sqrt{2} k_w m c^2}, \tag{4}$$

with e and m being the charge and mass of the electron, $\varepsilon_0 \approx 8.85 \times 10^{-12}\,\mathrm{F\,m^{-1}}$ being the vacuum permittivity, n_0 is the electron bunch density and $[JJ] = J_0\left[a_w^2/2\left(1 + a_w^2\right)\right] - J_1\left[a_w^2/2\left(1 + a_w^2\right)\right]$, where the dimensionless rms undulator parameter $a_w \equiv K/\sqrt{2}$.

For an electron bunch having both a linear chirp and a second-order curvature, i.e.,

$$\gamma = \gamma_0 + \left.\frac{\mathrm{d}\gamma}{\mathrm{d}t}\right|_{t=0} t_0 + \frac{1}{2}\left.\frac{\mathrm{d}^2\gamma}{\mathrm{d}t^2}\right|_{t=0} t_0^2 + \cdots, \tag{5}$$

the electron distribution can be linearized on

$$\psi_0 = \delta\big(p + \mu\theta_0 + \nu\theta_0^2/2\big) \tag{6}$$

with $\theta_0 = \theta - pZ$, and

$$\begin{cases} \mu = \left.\dfrac{\mathrm{d}\gamma}{\mathrm{d}t}\dfrac{2}{\gamma_0\omega_0}\right|_{t=0} \\ \nu = -\left.\dfrac{\mathrm{d}^2\gamma}{\mathrm{d}t^2}\dfrac{2}{\gamma_0\omega_0^2}\right|_{t=0}, \end{cases} \tag{7}$$

characterizing the energy chirp and the energy curvature in the electron bunch, respectively. Solving the Vlasov equation (2), and inserting the results in the Maxwell equation (3), assuming $\mu Z \ll 1$ and $\nu\theta Z \ll 1$, we have

$$\left(\frac{\partial}{\partial Z} + \frac{\partial}{\partial\theta}\right) A(\theta, Z) = \frac{D_1}{\gamma_0}\sum_j \mathrm{e}^{-\mathrm{i}\theta_j + \mathrm{i}(\mu\theta_j + \nu\theta_j^2/2)Z}\delta(\theta - \theta_j)$$
$$+\,\mathrm{i}(2\rho)^3\int_0^Z \mathrm{d}Z'(Z - Z')\,\mathrm{e}^{\mathrm{i}(\mu\theta + \nu\theta^2/2)(Z - Z')}A(\theta, Z'), \tag{8}$$

where $\theta_j = -\omega_0 t_j$ and $(2\rho)^3 = 2D_1D_2\big/\gamma_0^3$ with ρ being the Pierce parameter [8].

We introduce the Laplace transform

$$f(\theta, s) = \int_0^\infty \mathrm{d}Z\,\mathrm{e}^{-sZ}A(\theta, Z). \tag{9}$$

Equation (8) is then rewritten in the Laplace frequency domain as

$$\frac{\partial f(\theta, s)}{\partial\theta} + \left(s - \frac{\mathrm{i}(2\rho)^3}{[s - \mathrm{i}(\mu\theta + \nu\theta^2/2)]^2}\right) f(\theta, s)$$
$$= A(\theta, 0) + \frac{D_1}{\gamma_0}\sum_j \frac{\mathrm{e}^{-\mathrm{i}\theta_j}\delta(\theta - \theta_j)}{s - \mathrm{i}\big(\mu\theta_j + \nu\theta_j^2/2\big)}, \tag{10}$$

which yields the solution

$$f(\theta, s) = \int_{-\infty}^{\theta} \mathrm{d}\theta'\,\mathrm{e}^{-s(\theta - \theta') + K(\theta, \theta', s, \mu, \nu)}$$
$$\times\left[A(\theta', 0) + \frac{D_1}{\gamma_0}\sum_j \frac{\mathrm{e}^{-\mathrm{i}\theta_j}\delta(\theta' - \theta_j)}{s - \mathrm{i}\big(\mu\theta_j + \nu\theta_j^2/2\big)}\right], \tag{11}$$

where

$$K(\theta, \theta', s, \mu, \nu) = \int_{\theta'}^{\theta} \frac{\mathrm{i}(2\rho)^3}{[s - \mathrm{i}(\mu\theta'' + \nu\theta''^2/2)]^2}\,\mathrm{d}\theta''. \tag{12}$$

In the square bracket in equation (11), the first term $A(\theta', 0)$ characterizes the initial seed for a seeded FEL, while the second term models the shot noise source for the SASE FEL. Since we are considering only the seeded FEL, in the following we will keep only the term which depends on the initial seed, so equation (11) becomes

$$f(\theta, s) = \int_{-\infty}^{\theta} \mathrm{d}\theta'\,\mathrm{e}^{-s(\theta - \theta') + K(\theta, \theta', s, \mu, \nu)}A(\theta', 0). \tag{13}$$

The inverse Laplace transform gives the FEL field envelope along the undulator. After performing the contour integral first, the FEL field envelope can be written as the convolution of the initial seed with a Green's function

$$A(\theta, Z) = \int_0^\infty \mathrm{d}\xi\, A(\theta-\xi, 0)\mathcal{G}(\theta, \xi, Z, s), \tag{14}$$

with the Green's function $\mathcal{G}(\theta, \xi, Z, s)$ defined as

$$\mathcal{G}(\theta, \xi, Z, s) \equiv \int_c \frac{\mathrm{d}s}{2\pi i}\, \mathrm{e}^{s(Z-\xi)+K(\theta,\xi,s,\mu,\nu)}. \tag{15}$$

Note that due to the energy chirp and energy curvature in the electron bunch, the Green's function depends separately on ξ and θ, which are the FEL amplifier time variables, thus losing the translational invariance property. In general, for a Green's function without translation invariance, people normally decompose the Green's function into parts which have translation invariance and parts which break translation invariance. The part which breaks translation invariance normally is small and can be treated as perturbation, which usually describes local effects.

For convenience the integral representation in equation (14) is rewritten using the notation $\hat{z} = 2\rho Z$, $\hat{s} = \rho\theta$, $\hat{\xi} = \rho\xi$, $\hat{\alpha} = -\mu/(2\rho^2)$, $\hat{\beta} = \nu/(2\rho^3)$ and $\hat{p} = s/(2\rho)$, yielding

$$A(\hat{s}, \hat{z}) = \int_0^\infty \mathrm{d}\hat{\xi}\, A(\hat{s}-\hat{\xi}, 0) g(\hat{s}, \hat{z}, \hat{\xi}, \hat{\alpha}, \hat{\beta}), \tag{16}$$

and

$$g(\hat{s}, \hat{z}, \hat{\xi}, \hat{\alpha}, \hat{\beta}) = 2\int_c \frac{\mathrm{d}\hat{p}}{2\pi \mathrm{i}}\, \mathrm{e}^{\hat{\mathcal{F}}(\hat{p},\hat{s},\hat{z},\hat{\xi},\hat{\alpha},\hat{\beta})}, \tag{17}$$

where $\hat{\mathcal{F}}$ denotes the phasor

$$\hat{\mathcal{F}}(\hat{p}, \hat{s}, \hat{z}, \hat{\xi}, \hat{\alpha}, \hat{\beta}) = \hat{p}(\hat{z} - 2\hat{\xi}) + \hat{K}(\hat{p}, \hat{s}, \hat{z}, \hat{\xi}, \hat{\alpha}, \hat{\beta}). \tag{18}$$

Note that similar notation was adopted in [4].

2.2. *Exact expression of the Green's function*

The integral in equation (12) gives

$$K = \left.\frac{\mathrm{i}(2\rho)^3\left[\frac{\mu+\theta''\nu}{\mathrm{i}s+\theta''\mu+\theta''^2\nu/2} + \frac{2\nu\arctan\left(\frac{\mu+\theta''\nu}{\sqrt{2\mathrm{i}\nu s-\mu^2}}\right)}{\sqrt{2\mathrm{i}\nu s-\mu^2}}\right]}{\mu^2 - 2\mathrm{i}\nu s}\right|_{\theta''\to\theta'}^{\theta''\to\theta}. \tag{19}$$

Or according to equation (18),

$$\hat{K} = \left.\frac{2\mathrm{i}\left[\frac{\hat{s}''\hat{\beta}-\hat{\alpha}}{\mathrm{i}\hat{p}-\hat{s}''\hat{\alpha}+\hat{s}''^2\hat{\beta}/2} + \frac{2\hat{\beta}\arctan\left(\frac{\hat{s}''\hat{\beta}-\hat{\alpha}}{\sqrt{2\mathrm{i}\hat{\beta}\hat{p}-\hat{\alpha}^2}}\right)}{\sqrt{2\mathrm{i}\hat{\beta}\hat{p}-\hat{\alpha}^2}}\right]}{\hat{\alpha}^2 - 2\mathrm{i}\hat{\beta}\hat{p}}\right|_{\hat{s}''\to\rho\theta'}^{\hat{s}''\to\rho\theta}. \tag{20}$$

The Green's function describing the exponential growth can be evaluated by using the expression for $\hat{K}$ in equation (20) and numerically performing the integral in equation (17), choosing a closed anticlockwise path including the singularities, when $\hat{\xi} \neq 0$ and $\hat{\xi} < \hat{z}/2$.

The Green's function is crucial, since once the Green's function is known, the seeded FEL process is obtained based on the integral representation in equation (16), i.e., the seeded FEL is the convolution of the seed with the Green's function. To gain some insight to the seeded FEL process, in the following, we present an estimate of the Green's function analytically, but postpone the direct numerical evaluation based on the exact expression in equation (20) to a later subsection.

2.3. *Analytical approximation for the Green's function*

A closed analytical form for the Green's function is estimated by a saddle point approximation. The saddle point $\hat{p}_s$ is found as a solution of

$$\left.\frac{\mathrm{d}\hat{\mathcal{F}}(\hat{p})}{\mathrm{d}\hat{p}}\right|_{p=p_s} = 0 \tag{21}$$

with $\hat{\mathcal{F}}$ given in equation (18) and $\hat{K}$ in equation (20). At the saddle point, the phasor has the highest real part; therefore, for long undulators, the growth mode with the highest real part dominates the other ones. The Green's function is then approximated as

$$g(\hat{s},\hat{z},\hat{\xi},\hat{\alpha},\hat{\beta}) \approx \frac{2\exp[\hat{\mathcal{F}}(\hat{p}_s,\hat{s},\hat{z},\hat{\xi},\hat{\alpha},\hat{\beta})]}{[2\pi\hat{\mathcal{F}}''(\hat{p}_s,\hat{s},\hat{z},\hat{\xi},\hat{\alpha},\hat{\beta})]^{1/2}}. \tag{22}$$

As detailed in appendix A, to estimate $\hat{p}_s$, $\hat{\mathcal{F}}(\hat{p}_s)$ and $\hat{\mathcal{F}}''(\hat{p}_s)$ an order analysis is performed and the following expressions can be used to evaluate the Green's function:

$$\begin{aligned}
\hat{\mathcal{F}}(\hat{p}_s) = {} & \mathrm{i}^{\frac{1}{3}}\hat{z} - \frac{\mathrm{i}^{\frac{1}{3}}(\hat{z}-6\hat{\xi})^2}{4\hat{z}} + \frac{\mathrm{i}\hat{\alpha}}{2}(\hat{z}-2\hat{\xi})(\hat{\xi}-2\hat{s}) \\
& + \frac{\mathrm{i}\hat{z}\hat{\beta}}{36}\left(\frac{18\hat{\xi}\hat{z}-\hat{z}^2}{18} + (\hat{s}-\hat{\xi})(\hat{z}-6\hat{\xi}+12\hat{s})\right) + \frac{\mathrm{i}\hat{\beta}}{6}(\hat{z}-6\hat{\xi})(\hat{s}-\hat{\xi})^2 \\
& + \frac{\mathrm{i}^{\frac{5}{3}}\hat{z}^4}{432}\left(\frac{\hat{\alpha}^2}{\hat{z}} - \frac{\hat{\alpha}\hat{\beta}}{6} + \frac{\hat{z}\hat{\beta}^2}{135}\right) + \frac{\mathrm{i}^{-\frac{1}{3}}\hat{z}^2\hat{\beta}(\hat{s}-\hat{\xi})(12\hat{\alpha}\hat{\xi}-\hat{s}\hat{z}\hat{\beta})}{432} \\
& + \frac{\mathrm{i}^{-\frac{1}{3}}(\hat{z}-6\hat{\xi})\hat{z}^3}{432}\left(\frac{\hat{\alpha}^2}{\hat{z}} - \frac{\hat{\alpha}\hat{\beta}}{3} + \frac{\hat{z}\hat{\beta}^2}{45} + \frac{\hat{\beta}^2(\hat{s}-\hat{\xi})}{6}\right)
\end{aligned} \tag{23}$$

$$\begin{aligned}
\hat{\mathcal{F}}''(\hat{p}_s) = {} & -\frac{\mathrm{i}^{\frac{5}{3}}(5\hat{z}^2-24\hat{z}\hat{\xi}+36\hat{\xi}^2)}{\hat{z}} + \frac{\mathrm{i}\hat{z}^4}{108}\left(\frac{\hat{\alpha}^2}{\hat{z}} - \frac{\hat{\alpha}\hat{\beta}}{6} + \frac{\hat{z}\hat{\beta}^2}{135}\right) \\
& + \frac{\mathrm{i}\hat{z}^3\hat{\beta}(\hat{z}-6\hat{\xi})}{648}\left(\hat{\alpha} - \frac{4\hat{z}\hat{\beta}}{45}\right) + \frac{\mathrm{i}\hat{z}^3\hat{\beta}(\hat{s}-\hat{\xi})}{108}(\hat{s}\hat{\beta}-2\hat{\alpha}).
\end{aligned} \tag{24}$$

To further obtain a Green's function that yields a closed form when convoluted with a Gaussian seed laser, we rewrite equation (22) as

$$g(\hat{s},\hat{z},\hat{\xi},\hat{\alpha},\hat{\beta}) \approx \sqrt{\frac{2}{\pi}}\,\mathrm{e}^{\hat{\mathcal{F}}(\hat{p}_s,\hat{s},\hat{z},\hat{\xi},\hat{\alpha},\hat{\beta})-\frac{1}{2}\ln[\hat{\mathcal{F}}''(\hat{p}_s,\hat{s},\hat{z},\hat{\xi},\hat{\alpha},\hat{\beta})]}. \tag{25}$$

The expression of the exponential factor in equation (25) is given in equation (A.5).

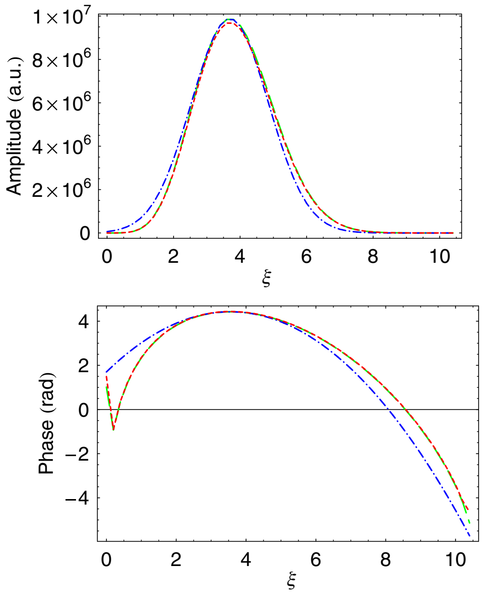

Figure 1. Comparison between the Green's function of equation (17) (dashed red line), that one of equation (22) numerically calculated (solid green line) and the same one obtained as the 3rd order saddle point approximation (dash-dotted blue line) for module (on the top) and phase (on the bottom).

Table 1. The parameters.

ρ	$\hat{\alpha}$	$\hat{\beta}$	γ	$\hat{z}$
0.005	0.0022	7.2×10^{-5}	2231	21

2.4. Comparison between the analytical and the numerical Green's functions

In order to evaluate the quality of the analytical treatment and the confidence degree of the assumption concerning the approximation, we perform a comparison between the exact Green's function obtained numerically in equations (17) and (20) and the equation derived from the saddle point approximation, see equation (25).

For this purpose, in figure 1 we consider a realistic set of parameters reported in table 1. These parameters are close to the design parameters of FERMI@Elettra project [9]. We plot the Green's function of equation (17) and that of equation (22) as a function of $\hat{\xi}$. This shows that the analytical approximation is in a very good agreement with the numerical solution, particularly close to the stationary phase condition, thus we continue to discuss the Green's function by using the analytical form.

3. Properties of the Green's function

The Green's function contains a time-independent contribution due to the undulator parameters and a time-dependent contribution coming from the chirp and curvature on the electron bunch energy, thus it depends on both variables $\hat{\xi}$ and $\hat{s}$ separately. The properties of the amplitude and phase of the Green's function strongly affect the characteristic of the FEL radiation along

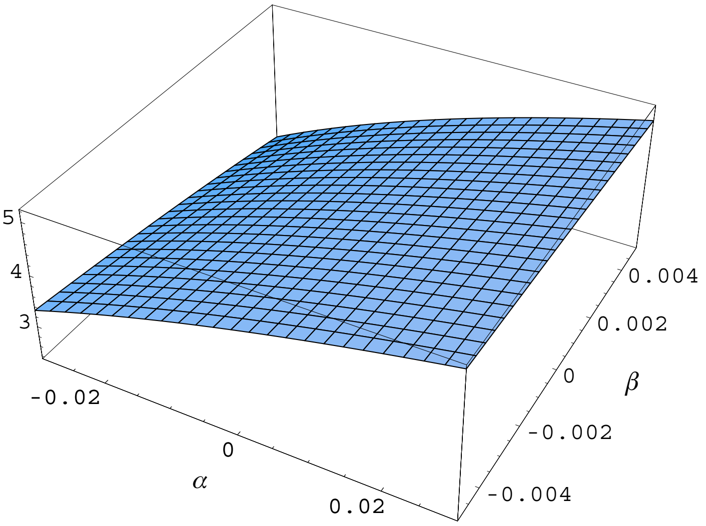

Figure 2. Position of the stationary phase point in $\hat{s}$ units with $\hat{z} = 25$ and $\hat{s} = \hat{z}/6$.

the undulator. Furthermore, the ratio between the Green's function temporal duration and the seed laser pulse temporal duration plays an important role as well. When the temporal duration of the seed laser is longer than that of the Green's function, the FEL radiation properties can be evinced directly by the Green's function. In particular, the central frequency shift and the frequency chirp of the FEL depend on the electron bunch time-dependent structure (i.e., on $\hat{\alpha}$ and $\hat{\beta}$). This will be reported in the accompanying paper [2]. Nevertheless, the study of the standing alone Green's function can give an insight into the characteristics of the FEL radiation independently of the seed temporal duration and shape. This will be the focus of the following sections in this paper.

The effects of a linear chirp and quadratic curvature on the real and imaginary part of the exponential factor in equation (A.5) are studied in appendix B. Both linear and quadratic terms have a small influence on the position of the amplitude peak of the Green's function (equation (B.3)), since $\hat{\alpha}$ and $\hat{\beta}$ only provide second-order term contributions. The linear chirp and the curvature affect much more the phase of the Green's function. The position of the stationary point of the phase is found according to equation (B.4), and it is plotted in figure 2 as a function of the chirp parameters.

To evaluate the shift and the chirp of the FEL central frequency, we have to calculate, respectively, the first and the second derivative in $\hat{s}$ of the phase of equation (16). Actually in the case of a seed laser much shorter than the Green's function (i.e. approaching the delta Dirac function), the FEL radiation is given straightforwardly by the Green's function and the derivation with respect to $\hat{s}$ equals the derivation with respect to $\hat{\xi}$ ($\partial\hat{\xi}/\partial\hat{s} \approx 1$). Thus to evaluate the shift of the FEL central frequency in this case, we consider the first derivative of the phase on $\hat{\xi}$ as in equation (B.5). We evaluate it in the maximum amplitude of the Green's function (i.e. $\hat{\xi} = \hat{\xi}_{Rpp}$ as expressed in equation (B.3)) choosing a delta function seed. Expanding to the first order in $\hat{\alpha}$ and $\hat{\beta}$, we obtain

$$\left.\frac{\partial I}{\partial \hat{\xi}}\right|_{\hat{\xi}=\hat{s}=\hat{\xi}_{Rpp}} \approx -\frac{\sqrt{3}}{\hat{z}} + \frac{\hat{z}}{2}\hat{\alpha} - \frac{\hat{z}^2}{36}\hat{\beta} + \frac{6-\sqrt{3}\hat{z}}{54}\hat{\beta}. \qquad (26)$$

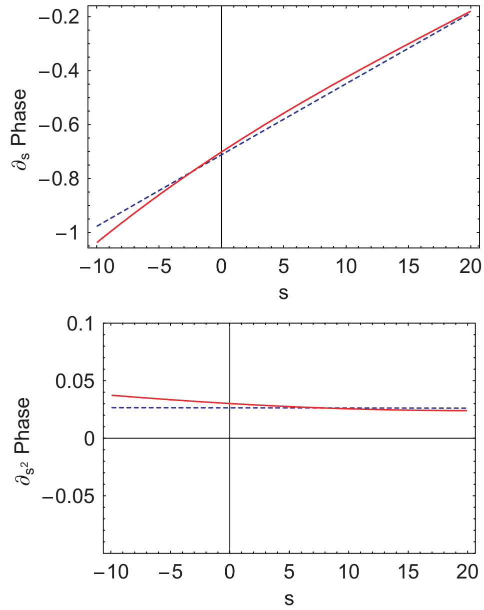

Figure 3. Comparison between the first (above) and the second (bottom) derivative of the integral in equation (16) (red solid line) for a long seed laser and the corresponding derivatives on $\hat{s}$ of the Green's function phase at its peak amplitude (blue dashed line).

The second derivative of the phase on $\hat{\xi}$ in equation (B.7) gives the radiation frequency chirp in the case of a short seed:

$$\left.\frac{\partial^2 I}{\partial \hat{\xi}^2}\right|_{\hat{s}=\hat{\xi}_{Rpp}} \approx -\frac{9}{\hat{z}} - 2\hat{\alpha} + \left(\frac{4}{3\sqrt{3}} + \frac{\hat{z}}{3}\right)\hat{\beta}. \tag{27}$$

In this configuration equation (27) shows that both the linear chirp and quadratic curvature have influence on the frequency chirp, but the main effect is due to the linear component. The first term is the intrinsic frequency chirp due to the FEL interaction [5]. The second term is inherited from the electron bunch energy chirp due to the resonant condition as in equation (1).

In contrast when the seed laser is longer than the Green's function, the former is almost constant in the convolution of equation (16) and the FEL radiation phase is mostly given by the phase of the Green's function amplitude peak. Thus the first and second derivatives on $\hat{s}$ of the FEL radiation phase are approximately given by the corresponding derivatives on $\hat{s}$ of the Green's function phase at its peak amplitude, as shown in figure 3. The first derivative of the phase on $\hat{s}$ in equation (B.6) evaluated in the corresponding maximum amplitude of the Green's function and expanded to the first order of $\hat{\alpha}$ and $\hat{\beta}$ is

$$\left.\frac{\partial I}{\partial \hat{s}}\right|_{\hat{\xi}=\hat{\xi}_{Rpp}} \approx \frac{\sqrt{3} - 3\hat{z}}{9} 2\hat{\alpha} - \frac{\sqrt{3}(12\hat{s} + \hat{z}) - 3\hat{z}(12\hat{s} - \hat{z}) - 4}{54}\hat{\beta}. \tag{28}$$

Considering the order analysis between $\hat{\alpha}$, $\hat{\beta}$ and $\hat{z}$, equation (28) shows that even if the quadratic curvature has influence on the central frequency shift, the main effect comes from the linear chirp. The second derivative of the Green's function phase on $\hat{s}$ is calculated in appendix B, and its value at the peak amplitude considering only the leading terms gives

$$\left.\frac{\partial^2 I}{\partial \hat{s}^2}\right|_{\hat{\xi}=\hat{\xi}_{Rpp}} \approx \frac{3z-\sqrt{3}}{9}2\hat{\beta} - z^2\frac{z-\sqrt{3}}{432}\hat{\beta}^2. \tag{29}$$

It is worthwhile to emphasize that regarding the FEL radiation frequency chirp, the energy curvature of the electrons becomes the main source of the frequency chirp in the case of a long seed according to equation (B.8).

Similarly to [5] we have calculated the temporal duration and the bandwidth of the Green's function:

$$\sigma^2_{t,\hat{\alpha},\hat{\beta}} = \frac{k_w z}{9\sqrt{3}\rho\omega_0^2}\frac{1}{1-2\eta}, \tag{30}$$

$$\sigma^2_{\omega,\hat{\alpha},\hat{\beta}} = \frac{3\sqrt{3}\rho\omega_0^2}{k_w z}\left(1+\frac{\kappa+\kappa^2+2\kappa\eta+4\eta^2}{1-2\eta}\right), \tag{31}$$

where

$$\eta = \frac{k_w^3 z^3\hat{\beta}\rho^3[-36\hat{\alpha}+\hat{\beta}(\sqrt{3}+6k_w z\rho)]}{2916}, \tag{32}$$

$$\kappa = \frac{2}{9}k_w z\hat{\alpha}\rho - \frac{10}{27}k_w^2 z^2\hat{\beta}\rho^2 + \frac{k_w^3 z^3\hat{\beta}^2\rho^3}{486\sqrt{3}} - \frac{4}{9}k_w z\hat{\beta}\rho^2(k_0 z - \omega_0 t). \tag{33}$$

Equation (30) reveals that the rms temporal duration is affected through the parameter η only by the energy curvature in the electron bunch, and this is a second-order effect. The Green's function bandwidth in equation (31) can be further simplified by neglecting 2η compared to 1 and third-order quantities in $\hat{\alpha}$ and $\hat{\beta}$ obtaining the following approximated expression:

$$\sigma^2_{\omega,\hat{\alpha},\hat{\beta}} = \frac{3\sqrt{3}\rho\omega_0^2}{k_w z}(1+\kappa+\kappa^2). \tag{34}$$

The FEL pulse travels with a group velocity [5] of $v_g = \omega_0/(k_0 + 2k_w/3)$, we have $k_0 z - \omega_0 t = -2k_w z/3$. The complete expression of the group velocity as a function of $\hat{\alpha}$ and $\hat{\beta}$ can be well approximated with the above expression since the terms in $\hat{\alpha}$ and in $\hat{\beta}$ are at least of the second order. So, the expression of κ in equation (32) can be simplified as

$$\kappa = \frac{2}{9}k_w z\hat{\alpha}\rho - \frac{2}{27}k_w^2 z^2\hat{\beta}\rho^2 + \frac{k_w^3 z^3\hat{\beta}^2\rho^3}{486\sqrt{3}}. \tag{35}$$

For the parameter set in table 1, this means that the Green's function bandwidth only increases by a factor of less than 0.3%.

4. Conclusion

The FEL Green's function for the case of an electron bunch having both an energy chirp and an energy curvature has been derived by solving the coupled Vlasov–Maxwell equations. The study of the obtained Green's function has revealed that the linear term of the electron energy chirp provides a shift in the FEL radiation frequency, and it is responsible for the radiation frequency chirp when the seed laser is much shorter than the Green's function temporal duration, and is close to a Dirac delta-function. Otherwise in the case of a longer seed laser, the energy curvature is mainly responsible for the frequency chirp of the FEL radiation. Moreover the energy curvature in the electron bunch influences the Green's function rms temporal duration. An approximated expression of the Green's function bandwidth as a function of $\hat{\alpha}$ and $\hat{\beta}$ was found.

Acknowledgments

The work of JW was supported by the Department of Energy, USA under contract DE-AC02-76SF00515. The work of JW was performed with the support of the Linac Coherent Light Source project at Stanford Linear Accelerator Center.

Appendix A. Green's function derivation

Since the expression in equation (12) is difficult to handle, it is expanded in a power series on μ and ν, and the phasor in equation (18) becomes

$$\hat{\mathcal{F}}(\hat{p},\hat{s},\hat{z},\hat{\xi},\hat{\alpha},\hat{\beta}) = \hat{p}(\hat{z}-2\xi) + \sum_{m=0}^{M}\left[\sum_{n=0}^{m}\frac{\mathrm{i}^{m+1}(m+1)!(\hat{s}^{2m-n+1}-(\hat{s}-\hat{\xi})^{2m-n+1})(-\hat{\alpha})^{n}\hat{\beta}^{m-n}}{n!(m-n)!(2m-n+1)2^{m-n-1}\hat{p}^{2+m}}\right] \tag{A.1}$$

To estimate $\hat{p}_s$ we introduce the slippage $\hat{\zeta}=\hat{z}-6\hat{\xi}$ and seed laser temporal duration $\hat{\eta}=\hat{s}-\hat{\xi}$. Then an order analysis is performed, fixing $\hat{\zeta}\sim\varepsilon, \hat{\eta}\sim 1, \hat{\alpha}\sim\varepsilon^2, \hat{\beta}\sim\varepsilon^3$ and $\hat{z}\sim\varepsilon^{-1}$. The saddle point $\hat{p}_s\approx\hat{p}_{s0}+\hat{p}_{s1}\varepsilon+\hat{p}_{s2}\varepsilon^2+\hat{p}_{s3}\varepsilon^3+\hat{p}_{s4}\varepsilon^4$ is obtained solving $d\hat{\mathcal{F}}(\hat{p})/d\hat{p}=0$ order-by-order in ε, and for this purpose we choose $M=5$ in equation (A.1). The approximated saddle point is found as

$$\begin{aligned}\hat{p}_s = {} & \mathrm{i}^{\frac{1}{3}} - \frac{\mathrm{i}^{\frac{1}{3}}(\hat{z}-6\xi)}{2\hat{z}} + \frac{\hat{\alpha}\mathrm{i}}{2}(\xi-2\hat{s}) + \frac{\mathrm{i}\hat{z}\hat{\beta}}{2}\left(-\frac{\hat{z}-12\xi}{108}+\frac{\hat{s}^2-\xi\hat{s}}{\hat{z}}\right) + \hat{\alpha}^2\frac{\mathrm{i}^{-\frac{1}{3}}\hat{z}(\hat{z}-18\xi)}{432} \\ & + \hat{\alpha}\hat{\beta}\frac{\mathrm{i}^{-\frac{1}{3}}\hat{z}^2}{108}\left(\hat{s}-\xi+\frac{10\xi-\hat{z}}{8}\right) + \frac{\mathrm{i}^{-\frac{1}{3}}\hat{z}^3\hat{\beta}^2}{216}\left(\frac{5\hat{z}-42\xi}{270}-\frac{\hat{s}-\xi}{6}-\frac{(\hat{s}-\xi)^2}{\hat{z}}\right) \\ & + \frac{\mathrm{i}^{\frac{1}{3}}\hat{z}^5}{46\,656}\left(\frac{\hat{\alpha}\hat{\beta}^2}{6}-\frac{\hat{\alpha}^2\hat{\beta}}{\hat{z}}-\frac{4\hat{\beta}^3\hat{z}}{567}\right) + \frac{\mathrm{i}^{\frac{1}{3}}\hat{z}^4}{23\,328}(\hat{s}-\xi)\left(\hat{\alpha}\hat{\beta}^2-\frac{\hat{z}\hat{\beta}^3}{12}\right) \\ & + \frac{\mathrm{i}\hat{z}^6}{62\,208}\left(\frac{\hat{\alpha}^4}{\hat{z}^2}-\frac{\hat{\alpha}^3\hat{\beta}}{3\hat{z}}+\frac{4\hat{\alpha}^2\hat{\beta}^2}{105}-\frac{13\hat{z}\hat{\alpha}\hat{\beta}^3}{7560}+\frac{\hat{z}^2\hat{\beta}^4}{42\,525}\right)\end{aligned} \tag{A.2}$$

Substituting it back into equation (A.1) and to the second derivative of the phasor, it yields the following expressions for the Green's function:

$$\begin{aligned}\hat{\mathcal{F}}(\hat{p}_s) = {} & +\frac{3\mathrm{i}^{\frac{1}{3}}(\hat{z}-2\hat{\xi})(\hat{z}+6\hat{\xi})}{4\hat{z}} + \frac{\mathrm{i}\hat{\alpha}}{2}(\hat{z}-2\hat{\xi})(\hat{\xi}-2\hat{s}) \\ & + \frac{\mathrm{i}\hat{z}\hat{\beta}}{36}\left[\frac{18\hat{\xi}\hat{z}-\hat{z}^2}{18}+(\hat{s}-\hat{\xi})(\hat{z}-6\hat{\xi}+12\hat{s})\right] + \frac{\mathrm{i}\hat{\beta}}{6}(\hat{z}-6\hat{\xi})(\hat{s}-\hat{\xi})^2 \\ & + \frac{\mathrm{i}^{\frac{5}{3}}\hat{z}^4}{432}\left(\frac{\hat{\alpha}^2}{\hat{z}}-\frac{\hat{\alpha}\hat{\beta}}{6}+\frac{\hat{z}\hat{\beta}^2}{135}\right) + \frac{\mathrm{i}^{-\frac{1}{3}}\hat{z}^2\hat{\beta}(\hat{s}-\hat{\xi})(12\hat{\alpha}\hat{\xi}-\hat{s}\hat{z}\hat{\beta})}{432} \\ & + \frac{\mathrm{i}^{-\frac{1}{3}}(\hat{z}-6\hat{\xi})\hat{z}^3}{432}\left[\frac{\hat{\alpha}^2}{\hat{z}}-\frac{\hat{\alpha}\hat{\beta}}{3}+\frac{\hat{z}\hat{\beta}^2}{45}+\frac{\hat{\beta}^2(\hat{s}-\hat{\xi})}{6}\right] \\ & + \frac{\hat{z}^4\hat{\beta}(\hat{z}-6\hat{\xi})\mathrm{i}^{\frac{1}{3}}}{699\,840}\left[15\hat{\alpha}^2-\frac{7\hat{z}\hat{\alpha}\hat{\beta}}{2}+\frac{4\hat{z}^2\hat{\beta}^2}{21}-\hat{z}\hat{\beta}^2(\hat{s}-\hat{\xi})\right] \\ & + \frac{\mathrm{i}^{\frac{1}{3}}\hat{z}^6}{58\,320}\left[-\frac{\hat{\alpha}^2\hat{\beta}}{2\hat{z}}+\frac{\hat{\alpha}\hat{\beta}^2}{12}-\frac{2\hat{z}\hat{\beta}^3}{567}+\frac{\hat{\beta}^2\hat{\alpha}(\hat{s}-\hat{\xi})}{\hat{z}}-\frac{\hat{s}\hat{\beta}^3(\hat{s}-\hat{\xi})}{2\hat{z}}\right]\end{aligned}$$

$$+\frac{\mathrm{i}\hat{z}^7(\hat{s}-\hat{\xi})}{46\,656}\left(-\frac{\hat{\alpha}^3\hat{\beta}}{\hat{z}^2}+\frac{\hat{\alpha}^2\hat{\beta}^2}{4\hat{z}}-\frac{2\hat{\alpha}\hat{\beta}^3}{105}+\frac{13\hat{z}\hat{\beta}^4}{30\,240}\right)$$
$$+\frac{\mathrm{i}\hat{z}^7}{186\,624}\left(\frac{\hat{\alpha}^4}{\hat{z}^2}-\frac{\hat{\alpha}^3\hat{\beta}}{3\hat{z}}+\frac{4\hat{\alpha}^2\hat{\beta}^2}{105}-\frac{13\hat{z}\hat{\alpha}\hat{\beta}^3}{7560}+\frac{\hat{z}^2\hat{\beta}^4}{42\,525}\right)$$
$$-\frac{\mathrm{i}^{-\frac{1}{3}}\hat{\beta}\hat{z}^9}{141\,087\,744}\left(\frac{10\hat{\alpha}^4}{\hat{z}^2}-\frac{10\hat{\alpha}^3\hat{\beta}}{3\hat{z}}+\frac{671\hat{\alpha}^2\hat{\beta}^2}{1620}-\frac{221\hat{z}\hat{\alpha}\hat{\beta}^3}{9720}+\frac{56\hat{z}^2\hat{\beta}^4}{120\,285}\right) \tag{A.3}$$

and

$$\hat{\mathcal{F}}''(\hat{p}_s)=-\frac{\mathrm{i}^{\frac{5}{3}}(5\hat{z}^2-24\hat{z}\hat{\xi}+36\hat{\xi}^2)}{\hat{z}}+\frac{\mathrm{i}\hat{z}^4}{108}\left(\frac{\hat{\alpha}^2}{\hat{z}}-\frac{\hat{\alpha}\hat{\beta}}{6}+\frac{\hat{z}\hat{\beta}^2}{135}\right)$$
$$+\frac{\mathrm{i}\hat{z}^3\hat{\beta}(\hat{z}-6\hat{\xi})}{648}\left(\hat{\alpha}-\frac{4\hat{z}\hat{\beta}}{45}\right)+\frac{\mathrm{i}\hat{z}^3\hat{\beta}(\hat{s}-\hat{\xi})}{108}(\hat{s}\hat{\beta}-2\hat{\alpha})$$
$$+\frac{\mathrm{i}^{-\frac{1}{3}}\hat{z}^6}{11\,664}\left[\frac{\hat{\alpha}\hat{\beta}^2}{6}-\frac{\hat{\alpha}^2\hat{\beta}}{\hat{z}}-\frac{4\hat{z}\hat{\beta}^3}{567}+\frac{\hat{\beta}^2(12\hat{\alpha}-\hat{z}\hat{\beta})(\hat{s}-\hat{\xi})}{6\hat{z}}-\frac{\hat{\beta}^3(\hat{s}-\hat{\xi})^2}{\hat{z}}\right]$$
$$+\frac{(\hat{z}-6\hat{\xi})\mathrm{i}^{-\frac{1}{3}}\hat{z}^5}{7776}\left(\frac{\hat{\alpha}^2\hat{\beta}}{\hat{z}}-\frac{5\hat{\alpha}\hat{\beta}^2}{18}+\frac{4\hat{z}\hat{\beta}^3}{243}\right)$$
$$+\frac{\mathrm{i}^{\frac{1}{3}}\hat{z}^5(\hat{s}-\hat{\xi})\hat{\beta}(\hat{z}\hat{\beta}-12\hat{\alpha})}{559\,872}\left(10\hat{\alpha}^2-\frac{5\hat{z}\hat{\alpha}\hat{\beta}}{3}+\frac{127\hat{z}^2\hat{\beta}^2}{3780}\right)$$
$$+\frac{\mathrm{i}^{\frac{1}{3}}\hat{z}^7}{93\,312}\left(\frac{5\hat{\alpha}^4}{\hat{z}^2}-\frac{5\hat{\alpha}^3\hat{\beta}}{3\hat{z}}+\frac{163\hat{\alpha}^2\hat{\beta}^2}{945}-\frac{127\hat{z}\hat{\alpha}\hat{\beta}^3}{22\,680}-\frac{\hat{z}^2\hat{\beta}^4}{127\,575}\right)$$
$$+\frac{\mathrm{i}\hat{z}^9}{839\,808}\left(\frac{\hat{\alpha}^4\hat{\beta}}{\hat{z}^2}-\frac{\hat{\alpha}^3\hat{\beta}^2}{3\hat{z}}+\frac{103\hat{\alpha}^2\hat{\beta}^3}{2520}-\frac{11\hat{z}\hat{\alpha}\hat{\beta}^4}{5040}+\frac{4\hat{z}^2\hat{\beta}^5}{93\,555}\right) \tag{A.4}$$

The terms with large denominators give small contributions to the Green's function and are cancelled in equations (23) and (24). It is interesting to find a Green's function that gives a closed form for the FEL radiation along the undulator when the initial seed is Gaussian. This is accomplished by approximating the exponential as $\hat{\mathcal{F}}''(\hat{p}_s)^{-1/2}$ obtaining equation (25). The term $+\frac{\mathrm{i}\hat{\beta}}{6}(\hat{z}-6\hat{\xi})(\hat{s}-\hat{\xi})^2$ in equation (A.3) has been expanded in a power series up to the second order from the stationary phase point of the unchirped Green's function $\hat{\xi}=\hat{z}/6$. Further the terms with powers of $\hat{\alpha}$ and $\hat{\beta}$ larger than 2, one has large denominators and their contribution to the Green's function can be neglected. From equation (22) the expression of the primitivable Green's function is

$$g(\hat{s},\hat{z},\hat{\xi},\hat{\alpha},\hat{\beta})\approx\frac{\mathrm{i}^{\frac{1}{6}}}{\sqrt{\pi\hat{z}}}\exp\left\{\mathrm{i}^{\frac{1}{3}}\hat{z}-\frac{\hat{z}-6\hat{\xi}}{2\hat{z}}-\frac{\mathrm{i}^{\frac{1}{3}}(\hat{z}-6\hat{\xi})^2}{4\hat{z}}+\frac{\mathrm{i}\hat{\alpha}}{2}(\hat{z}-2\hat{\xi})(\hat{\xi}-2\hat{s})\right.$$
$$+\frac{\mathrm{i}\hat{z}\hat{\beta}}{36}\left[\frac{18\hat{\xi}\hat{z}-\hat{z}^2}{18}+(\hat{s}-\hat{\xi})(\hat{z}-6\hat{\xi}+12\hat{s})\right]+\frac{\mathrm{i}(6\hat{s}-\hat{z})(\hat{z}-6\hat{\xi})\hat{\beta}}{216}(6\hat{s}+\hat{z}-12\hat{\xi})$$
$$-\frac{\mathrm{i}^{\frac{4}{3}}\hat{z}^3}{432}\left(\frac{\hat{\alpha}^2}{\hat{z}}-\frac{\hat{\alpha}\hat{\beta}}{6}+\frac{\hat{z}\hat{\beta}^2}{135}\right)\left(1-\mathrm{i}^{\frac{1}{3}}\hat{z}\right)+\frac{\mathrm{i}^{\frac{4}{3}}\hat{z}^2\hat{\beta}(\hat{s}-\hat{\xi})}{432}\left[2\hat{\alpha}-\hat{\beta}\hat{s}-\mathrm{i}^{\frac{1}{3}}(12\hat{\alpha}\hat{\xi}-\hat{\beta}\hat{s}\hat{z})\right]$$
$$\left.+\frac{\mathrm{i}^{\frac{4}{3}}\hat{z}^2(\hat{z}-6\hat{\xi})}{432}\left[\left(\frac{\hat{\alpha}^2}{\hat{z}}-\frac{\hat{\alpha}\hat{\beta}}{3}+\frac{\hat{z}\hat{\beta}^2}{45}\right)\left(1-\mathrm{i}^{\frac{1}{3}}\hat{z}\right)-\frac{\hat{\beta}^2(\hat{s}-\hat{\xi})}{6}\left(1+\mathrm{i}^{\frac{1}{3}}\hat{z}\right)\right]\right\}. \tag{A.5}$$

Appendix B. Green's function study

We give the expressions for the real (R) and imaginary (I) part of the exponential factor in equation (A.5), that are useful to discuss the properties of the Green's function,

$$
\begin{aligned}
R = {} & -\frac{1}{2} + \frac{3\hat{\xi}}{\hat{z}} + \frac{3\sqrt{3}(\hat{z}-2\hat{\xi})(\hat{z}+6\hat{\xi})}{8\hat{z}} - \hat{\alpha}^2\frac{\hat{z}(\sqrt{3}\hat{z}-1)\hat{\xi}}{144} \\
& + \frac{\hat{\alpha}\hat{\beta}\hat{z}^2}{144}\left\{\frac{1}{\sqrt{3}}\left[\hat{z}\hat{\xi} - \frac{\hat{z}^2}{12} + 6(\hat{s}-\hat{\xi})\hat{\xi}\right] + \frac{\hat{z}-12\hat{s}}{36}\right\} \\
& + \frac{\hat{\beta}^2\hat{z}^2}{288}\left[\frac{\hat{z}}{\sqrt{3}}\left(\hat{\xi}^2 - \hat{s}^2 + \frac{\hat{s}\hat{z}}{6} + \frac{2\hat{z}^2}{135} - \frac{3\hat{z}\hat{\xi}}{10}\right)\right. \\
& \left. + \frac{1}{3}\left(\hat{s}^2 + \frac{\hat{s}\hat{z}}{6} - \frac{2\hat{z}^2}{135} - 2\hat{s}\hat{\xi} - \frac{\hat{z}\hat{\xi}}{30} + \hat{\xi}^2\right)\right]
\end{aligned}
\tag{B.1}
$$

and

$$
\begin{aligned}
I = {} & \frac{3(\hat{z}-2\hat{\xi})(\hat{z}+6\hat{\xi})}{8\hat{z}} + \hat{\alpha}\frac{(\hat{z}-2\hat{\xi})(-2\hat{s}+\hat{\xi})}{2} \\
& + \hat{\beta}\left(\frac{\hat{s}^2\hat{z}}{2} + \frac{\hat{s}\hat{z}^2}{36} - \frac{\hat{z}^3}{162} - \hat{s}^2\hat{\xi} - \frac{5\hat{s}\hat{z}\hat{\xi}}{6} + \frac{\hat{z}^2\hat{\xi}}{12} + 2\hat{s}\hat{\xi}^2 - \frac{\hat{z}\hat{\xi}^2}{6}\right) \\
& + \hat{\alpha}^2\hat{z}\hat{\xi}\frac{\hat{z}-\sqrt{3}}{144} + \frac{\hat{\alpha}\hat{\beta}\hat{z}^3}{72}\left(\frac{\hat{z}-12\hat{\xi}}{72} - \frac{\hat{\xi}(\hat{s}-\hat{\xi})}{\hat{z}} + \frac{(12\hat{s}-\hat{z})}{24\sqrt{3}\hat{z}}\right) \\
& + \frac{\hat{\beta}^2\hat{z}^2}{864}\left[\hat{z}\left(\hat{s}^2 - \frac{\hat{s}\hat{z}}{6} - \frac{2\hat{z}^2}{135} + \frac{3\hat{z}\hat{\xi}}{10} - \hat{\xi}^2\right)\right. \\
& \left. + \sqrt{3}\left(2\hat{s}\hat{\xi} - \hat{s}^2 - \frac{\hat{s}\hat{z}}{6} + \frac{2\hat{z}^2}{135} + \frac{\hat{z}\hat{\xi}}{30} - \hat{\xi}^2\right)\right].
\end{aligned}
\tag{B.2}
$$

Both equation (B.1) and (B.2) are quadratic function of $\hat{\xi}$. The position of the peak of the real part which gives the maximum amplitude of the Green's function is found to be

$$
\hat{\xi}_{R\mathrm{pp}} = \left(\frac{1}{3\sqrt{3}} + \frac{\hat{z}}{6}\right)\left\{1 + \frac{-\frac{\hat{z}^2(-1+\sqrt{3}\hat{z})\hat{\alpha}^2}{216(2+\sqrt{3}\hat{z})} - \frac{\hat{z}^3(4-6\sqrt{3}\hat{s}+\sqrt{3}\hat{z})\hat{\alpha}\hat{\beta}}{648(2+\sqrt{3}\hat{z})} + \frac{\hat{z}^3[20\sqrt{3}-180\hat{s}+3\hat{z}(29+\sqrt{3}\hat{z})]\hat{\beta}^2}{116640(2+\sqrt{3}\hat{z})}}{1 - \frac{\hat{z}^3\hat{\beta}(-12\sqrt{3}\hat{\alpha}+\hat{\beta}+\sqrt{3}\hat{z}\hat{\beta})}{3888\sqrt{3}}}\right\}.
\tag{B.3}
$$

The position of the peak of the imaginary part which gives the stationary phase point is found to be

$$
\hat{\xi}_{I\mathrm{pp}} = \frac{\hat{z}}{6}\left\{1 + \frac{\frac{12\hat{s}+\hat{z}}{9}\hat{\alpha} + \frac{\hat{z}(-\sqrt{3}+\hat{z})}{216}\hat{\alpha}^2 + \frac{\hat{z}^2-36\hat{s}^2-6\hat{s}\hat{z}}{54}\hat{\beta} + \frac{\hat{z}^2(\hat{z}-6\hat{s})}{648}\hat{\alpha}\hat{\beta} - \frac{\hat{z}^2[\hat{z}(9\sqrt{3}+\hat{z})-60\sqrt{3}\hat{s}]\hat{\beta}^2}{38880}}{1 + \frac{2\hat{z}\hat{\alpha}}{9} + \frac{\hat{z}(\hat{z}-12\hat{s})}{27}\hat{\beta} - \frac{\hat{z}^3\hat{\alpha}\hat{\beta}}{324} + \frac{\hat{z}^3(\sqrt{3}+\hat{z})\hat{\beta}^2}{3888}}\right\}.
\tag{B.4}
$$

Both the linear chirp and the quadratic curvature have a minor influence on the position of the amplitude peak, because the main contribution factors to the expression in equation (B.3) are of the second order in $\hat{\alpha}$ and $\hat{\beta}$. Nevertheless chirps have a strong effect on the position of the imaginary part peak due to the first-order contribution.

To estimate the central frequency shift of the FEL radiation along the undulator, we consider the derivatives of I on $\hat{s}$ and $\hat{\xi}$. Derivatives on $\hat{\xi}$ will give information on the shift in the case of a seed much shorter than Green's function, while derivatives on $\hat{s}$ will give information when the seed is longer than the Green's function.

$$\frac{\partial I}{\partial \hat{\xi}} = \frac{3}{2} - \frac{9\hat{\xi}}{\hat{z}} + \frac{\hat{\alpha}(4\hat{s} + \hat{z} - 4\hat{\xi})}{2} + \frac{\hat{\beta}(\hat{z}^2 + 48\hat{s}\hat{\xi} - 4\hat{z}\hat{\xi} - 12\hat{s}^2 - 10\hat{s}\hat{z})}{12} + \frac{\hat{\alpha}^2\hat{z}(\hat{z} - \sqrt{3})}{144} - \frac{\hat{\alpha}\hat{\beta}\hat{z}^2(6\hat{s} + \hat{z} - 12\hat{\xi})}{432} + \frac{\hat{z}^3\hat{\beta}^2}{144}\left(\frac{\hat{s} - \hat{\xi}}{\hat{z}\sqrt{3}} + \frac{\sqrt{3} + 9\hat{z} - 60\hat{\xi}}{180}\right), \tag{B.5}$$

$$\frac{\partial I}{\partial \hat{s}} = -\hat{\alpha}(\hat{z} - 2\hat{\xi}) + \hat{\beta}\left[\hat{s}(\hat{z} - 2\hat{\xi}) + \frac{\hat{z}^2}{36} - \frac{5\hat{z}\hat{\xi}}{6} + 2\hat{\xi}^2\right] + \frac{\hat{z}^2\hat{\alpha}\hat{\beta}(\sqrt{3} - 6\hat{\xi})}{432} + \frac{\hat{z}^2\hat{\beta}^2}{144}\left[\frac{1}{\sqrt{3}}\left(\hat{\xi} - \hat{s} - \frac{\hat{z}}{12}\right) + \frac{\hat{s}\hat{z}}{3} - \frac{\hat{z}^2}{36}\right]. \tag{B.6}$$

For the frequency chirp in the FEL radiation, we consider the second derivatives of the phase on $\hat{s}$ and $\hat{\xi}$, obtaining the expressions

$$\frac{\partial^2 I}{\partial \hat{\xi}^2} = -\frac{9}{\hat{z}} - 2\hat{\alpha} + \left(4\hat{s} - \frac{\hat{z}}{3}\right)\hat{\beta} + \frac{\hat{z}^2\hat{\alpha}\hat{\beta}}{36} - \frac{\sqrt{3} + \hat{z}}{432}\hat{\beta}^2\hat{z}^2 \tag{B.7}$$

and

$$\frac{\partial^2 I}{\partial \hat{s}^2} = \hat{\beta}(\hat{z} - 2\hat{\xi}) + \frac{\hat{z} - \sqrt{3}}{432}\hat{z}^2\hat{\beta}^2. \tag{B.8}$$

Equations (B.7) and (B.8) show that a short seed will have a strong intrinsic chirp, and its frequency chirp will be more affected by the linear chirp of the energy electron bunch than by the curvature. In contrast the frequency chirp in the case of a longer seed will mostly depend on the curvature of the electron bunch energy.

References

[1] Akre R *et al* 2008 *Phys. Rev. ST Accel. Beams* **11** 030703

[2] Craievich P, Lutman A, Penco G and Wu J 2008 Impact of an initial energy chirp and an initial energy curvature on a seeded free electron laser: free electron laser properties (in preparation)

[3] Krinsky S and Huang Z 2003 Frequency chirped self-amplified spontaneous-emission free-electron lasers *Phys. Rev. ST Accel. Beams* **6** 050702

[4] Saldin E L, Schneidmiller E A and Yurkov M V 2006 Self-amplified spontaneous emission FEL with energy-chirped electron beam and its application for generation of attosecond x-ray pulses *Phys. Rev. ST Accel. Beams* **9** 050702

[5] Wu J, Murphy J B, Emma P J, Wang X, Watanabe T and Zhong X 2007 Interplay of the chirps and chirped pulse compression in a high-gain seeded free-electron laser *J. Opt. Soc. Am.* B **24** 484

[6] Wu J, Bolton P R, Murphy J B and Wang K 2007 ABCD formalism and attosecond few-cycle pulse via chirp manipulation of a seeded free electron laser *Opt. Express* **15** 12749

[7] Wang J-M and L-H Yu 1986 A transient analysis of a bunched beam free electron laser *Nucl. Instrum. Methods Phys. Res.* A **250** 484

[8] Bonifacio R, Pellegrini C and Narducci L M 1984 Collective instabilities and high-gain regime in a free-electron laser *Opt. Commun.* **50** 373–8

[9] The Conceptual Design Report (CDR) for the FERMI@Elettra project Synchrotron Trieste *Technical Report* ST/F-TN-07/12 2007